International Journal of Pharmaceutics 439 (2012) 207–215

Contents lists available at SciVerse ScienceDirect

International Journal of Pharmaceutics

journal homepage: www.elsevier.com/locate/ijpharm

Pharmaceutical nanotechnology

Insights into the multi-equilibrium, superstructure system based on β-cyclodextrin and a highly water soluble guest

Elgte Elmin B. De Paula[a,b], Frederico B. De Sousa[b], Júlio César C. Da Silva[b], Flaviana R. Fernandes[c], Maria Norma Melo[c], Frédéric Frézard[c], Richard M. Grazul[a], Rubén D. Sinisterra[b], Flávia C. Machado[a,*]

[a] Núcleo de Espectroscopia e Estrutura Molecular, Departamento de Química, Universidade Federal de Juiz de Fora, Campus Universitário s/n, Martelos, Juiz de Fora, MG, 36036-900, Brazil
[b] Laboratório de Encapsulamento Molecular e Biomateriais, Departamento de Química – ICEx, Universidade Federal de Minas Gerais, Belo Horizonte-MG, 31270-901, Brazil
[c] Departamento de Fisiologia e Biofísica, Instituto de Ciências Biológicas, Universidade Federal de Minas Gerais, Belo Horizonte, Minas Gerais, Brazil

ARTICLE INFO

Article history:
Received 2 July 2012
Received in revised form 3 September 2012
Accepted 17 September 2012
Available online 25 September 2012

Keywords:
Supramolecular complex
β-cyclodextrin
Pentamidine
Multi-equilibrium
Leishmaniasis
In vivo experiments

ABSTRACT

Pentamidine isethionate (PNT) is an antiprotozoal active in many cases of leishmaniasis, despite the present limitations including high toxicity and parenteral administration. In the present work, a PNT encapsulation strategy into β-cyclodextrin cavity at 1:1 and 2:1 (βCD:PNT) molar ratios was used in order to improve the drug's physical and chemical properties. Combining thermodynamic and structural approaches such as isothermal titration calorimetry (ITC), electrospray ionization mass spectrometry (ESI-MS) and nuclear magnetic resonance (^{1}H NMR, and ROESY) the inclusion process and the thermodynamics parameters were identified. ITC and ESI-MS experimental data suggest the simultaneous formation of different supramolecular complexes in solution. Moreover, NMR data are in accordance with these results, suggesting a deep inclusion of PNT into the βCD cavity, through correlations observed in 2D ROESY contour maps. The systems were also characterized by FTIR, TG/DTA and SEM. These techniques indicate the formation of inclusion complex in the solid state. *In vivo* PNT activity was evaluated orally in mice. The inclusion complex showed a significant reduction of parasite load compared to free PNT.

1. Introduction

Leishmaniasis is one of the most neglected tropical diseases which is caused by an intracellular protozoan parasite belonging to the genus *Leishmania* (Akopyants et al., 2009). Chemotherapy of infected patients with Leishmaniasis still represents a serious problem, as the treatment options are very limited (Croft et al., 2005; Murray et al., 2005). The first choice drugs for treatment are based on pentavalent antimony, however, these have limited efficacy and significant toxicity (Nakayama et al., 2005). In particular, 1,5-bis(4-amidinophenoxy)pentane isethionate, Pentamidine (PNT) depicted in Fig. 1a first synthesized in the 40s (Ashley et al., 1942), is a well known aromatic diamidine with antiprotozoan activity. PNT is commonly used as second-line antileishmanial drug (Nacher et al., 2001; Croft and Yardley, 2002) and is most recommended in case of antimonial resistant (Croft and Yardley, 2002; Nakayama et al., 2005) or, more recently, in cases of cross-infection with HIV (Manfredi et al., 2008). An important feature of this drug is based on the fact that at physiological pH the amidine groups are protonated, which decreases the drug's permeability, thereby reducing its oral activity (Docampo and Moreno, 2003). Thus, PNT requires a parenteral administration, which makes the treatment less practical, especially in more isolated areas, where treatment access is difficult (Nakayama et al., 2005).

PNT is well tolerated by most patients in spite of some reported adverse effects, including nephrotoxicity, hepatotoxicity and hypotension (Puckowska et al., 2004; Nakayama et al., 2005; Zolek and Maciejewska, 2010). These adverse effects associated with the increasing resistance of the protozoa to PNT require sophisticated approaches to delivery of this class of drugs. Efficient alternatives include chemical modification to obtain drug analogues or using modified drug delivery systems. In particular, molecular encapsulation has been applied to many classes of drugs and the observed results have been promising, indicating an improvement in the physical, chemical and biological properties of the included molecules (Marques et al., 2011; Passos et al., 2011). Previous works have reported the PNT encapsulation in liposomes (Banerjee et al., 1996; Siddiqui et al., 2009) and nanoparticles (Paul et al., 1997, 1998) in order to increase tolerance and to reduce drawbacks. Particularly, drug encapsulation into cyclodextrins (CDs) cavities is an interesting alternative that has been applied to a variety of guest drugs, being these macromolecules good candidates for sophisticated drug delivery systems (De Sousa et al., 2010; Ivana Lula et al., 2011).

* Corresponding author. Tel.: +55 32 2102 3310; fax: +55 32 2102 3314.
E-mail address: flavia.machado@ufjf.edu.br (F.C. Machado).

0378-5173
http://dx.doi.org/10.1016/j.ijpharm.2012.09.039

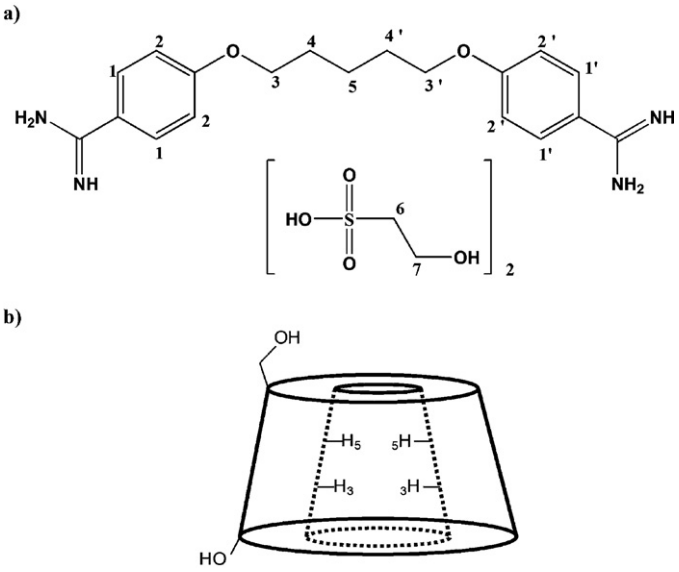

Fig. 1. Schematic structure of (a) Pentamidine isethionate and (b) β-cyclodextrin.

It is well known that CDs are cyclic oligosaccharides with a truncated cone shape as shown in Fig. 1b, formed by 6, 7, or 8 glucopyranose units linked by α-1,4-glycosidic bond, respectively named as α-, β-, or γ-cyclodextrin. The polar hydroxyl groups located on the molecule's border confer water solubility, while, their hydrophobic cavity allows them to host a variety of "guest" molecules, forming inclusion complexes (ICs) which are stabilized by non covalent interactions, this amphiphilic character being the main characteristic of CDs (Szejtli, 1998; Wenz et al., 2006). CDs are used as multi-functional pharmaceutical excipients due to their special ability to complex drugs, modifying their properties such solubility, stability, bioavailability and toxicity (Loftsson et al., 2005; Brewster and Loftsson, 2007; Carrier et al., 2007).

It has been previously described in the literature that in aqueous solutions, CDs and their ICs are able to self-assemble, forming superstructures (Messner et al., 2010; De Sousa et al., 2012). CDs can assemble into different aggregates under specific condition (He et al., 2008), which are in dynamic equilibrium with free molecules (Duan et al., 2005), these assembled structures being stabilized by hydrophobic, van der Waals, hydrogen bonding, and electrostatic interactions (Lehn, 2002). Since not only a host–guest interactions would need to be broken, but a large number hydrogen bonding and other attractive forces should be disrupted to release the drug molecule, being assembled superstructures an additional reason for the modified drug release profile (Chen and Liu, 2010; De Sousa et al., 2012). In this sense, several physical-chemical techniques have been used in order to identify these assembled superstructures in the presence and absence of guest molecules, correlating system size, structure, morphologies and biological activity of the drugs (Duan et al., 2005; He et al., 2008; Chen and Liu, 2010; Messner et al., 2010; De Sousa et al., 2012).

Therefore, the aim of this study is to investigate the inclusion of PNT into the βCD cavity and the influence of the host molecule concentration in the supramolecular structure and assembly properties. Additionally, the inclusion process in βCD can turn PNT active by oral administration resulting in a feasible and accessible treatment. ICs were characterized by isothermal titration calorimetry (ITC), electrospray ionization-mass spectrometry (ESI-MS) and nuclear magnetic resonance (uni and bi-dimensional experiments). PNT inclusion was also characterized in the solid state by Fourier transform infrared spectroscopy (FTIR), thermal analysis (TG and DTA) and scanning electron microscopy (MEV). In order to evaluate our assumptions about the CDs superstructures, orally *in vivo* experiments were performed to verify the antileishmanial activity of the included drug.

2. Materials and methods

2.1. Reagents and inclusion compounds preparation

PNT and βCD were obtained from Sigma Aldrich and Roquette, respectively. All ICs were prepared by a freeze-drying method at 1:1, 2:1, 3:1 and 4:1 molar ratios of βCD:PNT. In this method, an aqueous solution (50 mL) containing PNT (1.69×10^{-3} mol/L for all molar ratios) and βCD (1.69×10^{-3}, 3.37×10^{-3}, 5.06×10^{-3} and 6.74×10^{-3} mol/L for 1:1, 2:1, 3:1 and 4:1 molar ratios of βCD:PNT, respectively) was stirred for 8 h to ensure that equilibrium had been obtained. The resulting solution was frozen in liquid nitrogen and lyophilized for 72 h to obtain the solid ICs. In order to compare the results in the solid state, physical mixtures (PMs) were prepared in the same molar ratios of those ICs, PM-βCD:PNT (1:1), PM-βCD:PNT (2:1), PM-βCD:PNT (3:1) and PM-βCD:PNT (4:1).

2.2. Isothermal titration calorimetry experiments

Calorimetric titrations were performed in a VP-ITC Microcalorimeter (Microcal Company, Northampton, MA, USA) at 25 °C. Each titration experiment consisted of 50 successive injections of PNT aqueous solution (30.0 mmol L^{-1}) into the reaction cell loaded with 1.5 mL of a βCD aqueous solution (1.0 mmol L^{-1}), with time intervals of 230 s, which were sufficiently long for the signal to return to the baseline. The first injection of 1 μL was discarded to eliminate diffusion effects of material from the syringe in the calorimetric cell. Subsequent injections of constant volume of 5 μL of PNT were carried out with an injection time of 5 s. PNT heat of dilution was studied in the control experiment to be subsequently subtracted from the heat reaction measured in the titration of PNT in βCD aqueous solution, to achieve the net heat of reaction.

Data were collected automatically and subsequently analyzed by the software package supplied by the calorimeter (Microcal Origin 5.0 for ITC). Stoichiometry (N), binding constant (K) and enthalpic contribution (ΔH°) were obtained by nonlinear fitting incorporated in the software (one binding site model). From these results, the change in Gibbs standard free energy (ΔG°) was calculated using the binding constant and the entropic contribution was subsequently calculated.

2.3. Nuclear magnetic resonance experiments

NMR spectra were recorded at 27 °C in a Bruker DRX 400 AVANCE spectrometer (Bruker BioSpin, Rheinstetten, Germany) operating at 400 MHz, equipped with a 5 mm inverse probe with a z-gradient coil. ^{1}H NMR spectra were acquired using the WATERGATE technique for residual water signal suppression (Piotto et al., 1992; Sklenar et al., 1993). Nuclear rotating frame Overhauser enhancement spectroscopy (2D ROESY) experiments (mixing time 400 ms) were acquired using standard experiments from the spectrometer library. PNT and its ICs at all molar ratios were dissolved in D_2O (Cambridge Isotope Laboratories, Inc. 99.9% of isotopic purity).

2.4. Electrospray ionization mass spectrometry (ESI-MS)

The anti-leishmanial PNT and its ICs with various PNT:βCD stoichiometric ratios were investigated by ESI-MS. This technique has been applied to study similar systems (Martins et al., 2006; Denadai et al., 2007) providing insights about the supramolecular structure of the ICs, including the assembly process and stoichiometry.

ESI-MS analyses were conducted using an MS instrument (model LCQ-Fleet, Thermo-Scientific, San Jose, CA, USA) coupled to an ion trap analyzer and operating in the positive ion mode. Aliquots of 500 μL aqueous solutions were directly injected within the ion source by means of a microsyringe. The concentration of PNT analyzed was 0.0127 mol/L and of ICs were 5.83×10^{-3}, 3.50×10^{-3}, 2.53×10^{-3} and 2.11×10^{-3} mol/L for 1:1, 2:1, 3:1 and 4:1 molar ratios of βCD:PNT, respectively. Typical conditions were used as follow: microsyringe flow rate of 20 μL min^{-1}; capillary temperature of 275 °C; capillary and cone voltages 16 V and of 5 kV, respectively. Each mass spectrum, acquired in the *m*/*z* range of 50–2000, was obtained as an average of 50 scans, each one requiring 0.1 s.

2.5. Fourier transform infrared spectroscopy (FTIR)

Infrared spectra were obtained with a Bomen MB-102 spectrometer using KBr pellets in the wavenumber range of 4000–400 cm^{-1} at a resolution of 4 cm^{-1}. Good signal-to-noise ratios were obtained from accumulation of 64 scans.

2.6. Thermal analysis (TG and DTA)

Thermogravimetric analysis (TG) and differential thermal analysis (DTA) were executed on a TA instruments SDT Q600 using a nitrogen gas purge atmosphere at 50 mL min^{-1} and a heating rate of 10 °C min^{-1}. All compounds (about 6 mg) were analyzed in a range from 25 to 700 °C in an open alumina pan (Al_2O_3) and an empty alumina pan was used as reference. DTA curves of free molecules, PMs and ICs were obtained simultaneously with the TG experiments.

2.7. Scanning electron microscopy (SEM)

Morphologies of βCD, PNT, PMs and ICs, coated with thin gold layer, were analyzed using scanning electron microscopy in a JEOL, Mod JSM 840A microscope, operating at 4–10 kV.

2.8. In vivo experiments

2.8.1. Parasites

Leishmania (L.) *infantum chagasi* (MHOM/BR/70/BH46) parasites were routinely maintained and isolated from Golden Syrian hamsters (*Mesocricetus auratus*) and were grown as promastigotes at 26 °C in Dulbecco Modified Eagle medium (DMEM, Sigma), supplemented with 20% heat-inactivated fetal bovine serum (FBS, Cultilab, Brazil), 2 mmol L^{-1} L-glutamine, 25 mmol L^{-1} HEPES, 50 mmol L^{-1} 2-mercaptoethanol and 20 mg mL^{-1} of gentamycin, at pH 7.0.

2.8.2. Mice infection and treatment protocol

BALB/c mice (female, 4–6 week-old) were obtained from Cebio (Centro de Bioterismo do Instituto de Ciências Biológicas, Universidade Federal de Minas Gerais). Free access was allowed to standard diet and tap water was supplied *ad libitum*.

Groups of mice ($n = 7$–10) were infected in the tail vein with 1×10^6 of late log phase *L.* (L.) *infantum chagasi* promastigotes. The treatment was started 8 days after infection with daily doses for 20 days. The different formulations administered by gavage with doses of 200 μL, to mice of five groups, was as follows: the first group was treated with free PNT in a dose of 50 mg/kg (8.85×10^{-3} mol/L), the second group with the βCD:PNT at 1:1 (9.43×10^{-3} mol/L) in a dose of 145 mg/kg (which contains the same mass of the free drug used in the first group), the third was treated with free βCD (8.02×10^{-3} mol/L) at a dose of 95 mg/kg (same dosage of βCD presented in the IC at 1:1) and a fourth group was treated with saline (negative control). A fifth group used as positive control, received the commercial antimonial drug Glucantime® (Sanofi-Aventis, São Paulo, Brazil), intraperitoneally at 80 mg/kg. All groups were treated daily and after 21 days, the animals were sacrificed and the spleen and liver were harvested for determination of parasite burdens.

Experimental protocols were performed in accordance with the guidelines for the humane use of laboratory animals and received approval from the Ethics Committee in Animal Experimentation of the Federal University of Minas Gerais (protocol no. 199/2011).

2.8.3. Parasite quantification

Liver and spleen were collected to determine the parasite burdens in mice challenged with *L. chagasi*, as previously described (Marques-da-Silva et al., 2005). Briefly, organs were weighed, fragmented and a tissue homogenate was obtained in 1 mL of DMEM plus 20% FBS, at pH 7.0. Five-fold serial dilutions were performed in 96-well flat-bottom microtiter plates (Nunc, Nunclon), in duplicate, and plates were incubated at 23 °C. Plates were evaluated for parasite growth using a microscope (Axiovert 25, Zeiss). The number of viable parasites was determined from the highest dilution at which promastigotes had grown, after 12 days of incubation.

3. Results and discussion

3.1. Isothermal titration calorimetry

ITC is a powerful technique to study the complexation process in supramolecular systems. Thus, it was used in order to evaluate the thermodynamic parameters of the supramolecular interaction between PNT and βCD. Fig. 2a shows the PNT titration in water (control experiment) and in βCD aqueous solution while Fig. 2b shows the heat of reaction measured in the titration of PNT in βCD aqueous solution, after subtracting the heat of dilution of PNT in water.

PNT dilution experiment in water demonstrates a slightly exothermic profile (Fig. 2a), which can be correlated with the dissociation of the PNT molecules in the reaction cell. The PNT titration curve in βCD provides negative heat of reaction values, indicating an exothermic process, as observed in Fig. 2b. This exothermic profile can be attributed to the host–guest interactions as described for similar systems (Denadai et al., 2007; De Sousa et al., 2008b). This curve was fitted using the nonlinear adjustment based on the Wiseman isotherm (Turnbull and Daranas, 2003), providing the stoichiometric coefficient (N) equivalent to 0.84 ± 0.01, the equilibrium constant $K = 758 \pm 7$ and the enthalpy contribution $\Delta H^\circ = -11.2 \pm 0.2$ kJ mol^{-1}. Furthermore, the PNT:βCD IC formation process was spontaneous as evidenced by the Gibbs standard free energy ΔG° (-16.4 kJ mol^{-1}). Additionally, a positive entropic contribution ($T\Delta S^\circ = 5.2$ kJ mol^{-1}) was calculated.

Complexation thermodynamic parameters reflect the nature of non covalent interactions occuring between guest and host molecules. The ICs formation is primarily a result of hydrophobic interactions between the guest molecule and the host's relatively hydrophobic cavity; therefore, it is driven by the enthalpic contribution. Enthalpy change can be associated with the water molecules exit from the βCD cavity to accommodate the PNT molecule and the formation of supramolecular cooperative interactions between the drug and the host molecule. The desolvation of βCD and PNT during the complexation can be an important contribution to the positive entropic component, through the gain of rotational and translational entropy of water molecules released when compared to the pure substances. The N value suggests different equilibria between supramolecular systems in solution and is in agreement with other results previously reported (Denadai et al., 2007; De Sousa et al., 2008b).

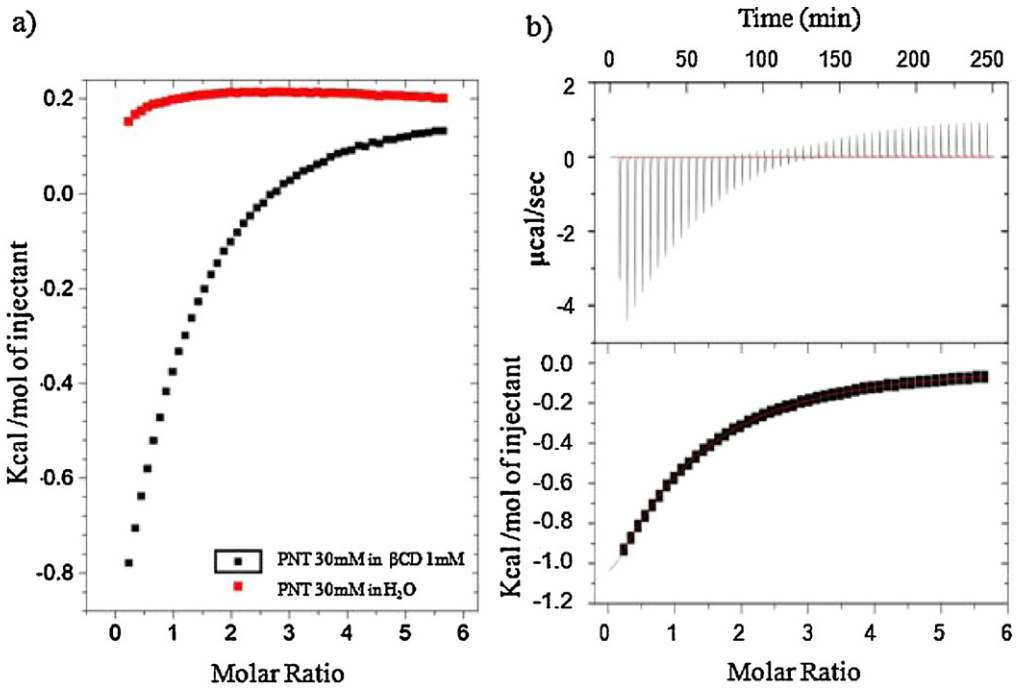

Fig. 2. (a) ITC experiments for PNT, 30.0 mmol L^{-1} in water (■) and in βCD 1.0 mmol L^{-1} (■). (b) Final figure: (-) raw data, (■) subtracted curve of titration, (- - -) nonlinear regression.

3.2. Nuclear magnetic resonance studies

^{1}H NMR spectra of βCD:PNT complexes at different molar ratios (1:1, 2:1, 3:1 and 4:1) were obtained in D_2O solution and can be viewed in the Supplementary Material (Fig. S1). Hydrogen chemical shift for free PNT and its ICs at 1:1 and 2:1 molar ratio, as well as, the chemical shifts variation ($\Delta\delta = \delta_{PNT} - \delta_{\beta CD:PNT}$) are summarized in Table 1. Changes in PNT chemical shift were observed in presence of βCD, when compared to the free PNT (Charpentier et al., 2008). These changes emphasize the interactions between the drug and the host molecules, as these shifts are associated with changes in electron density due to the inclusion of PNT into the βCD cavity (Schneider et al., 1998; De Sousa et al., 2008c). In spite of the βCD:PNT molar ratio (1:1 or 2:1), the most affected PNT hydrogens are H1 of the aromatic moiety and the H5 aliphatic portion, suggesting a deep inclusion into the βCD cavity. On the other hand, the less affected PNT hydrogens are H6 and H7 from isethionate group, indicating that this group does not participate in the inclusion process. Additionally, the ^{1}H NMR spectra of βCD:PNT at 3:1 and 4:1 showed no significant difference from the ^{1}H NMR spectrum at 2:1, indicating that increasing the concentration above the 2:1 ratio did not lead to different superstructures in aqueous solution.

In addition to the analysis of the chemical shift variations, Nuclear Overhauser Effect (NOE) experiments have been successfully applied to illustrate the through-space intermolecular interaction, these measurements being one of the most important tools to confirm the guest inclusion into the βCD cavity. This experiment shows cross peak correlations among hydrogens indicating interactions at a short distance (less than 5 Å), (Schneider et al., 1998; Gibaud et al., 2005) due to electromagnetic dipolar coupling (Teixeira et al., 2006). The 2D ROESY spectrum of the βCD:PNT (1:1) supramolecular system is shown in Fig. 3, in which several cross peaks correlation are observed between PNT hydrogens and those from βCD (H-3 and H-5 internal and H-2 and H-4 external). Fig. 3b and c shows the 2D ROESY contour map expansions with the main cross peaks correlations between βCD and PNT.

Cross peaks correlations between aromatic hydrogens (H1 and H2) and the aliphatic protons (H4 and H5) of PNT with the H-3 and H-5 internal hydrogens of the βCD cavity, can be observed. Moreover, cross peak correlations between H6 and H7 from isethionate and H-4 and H-2 from βCD may also be observed.

These results confirm the deep inclusion of PNT into the βCD cavity, in which not only the aromatic moiety is included as usual (Denadai et al., 2007; De Sousa et al., 2008a), but also the aliphatic chain is placed inside the βCD cavity. In addition, the 2D ROESY results are in agreement with the ^{1}H NMR experiments, which indicated the interaction of the isethionate group with βCD outer side leading to the smaller chemical shifts variations.

3.3. ESI-MS studies

ESI-MS in the positive mode (ESI(+)-MS) was used to gain insights about the supramolecular species distribution in aqueous solutions at the following βCD:PNT molar ratio 1:1, 2:1, 3:1, and 4:1, Fig. 4a, b, c and d, respectively. The ESI(+)-MS spectrum of the free PNT is presented as Supplementary Material (Fig. S2).

Fig. 4a show ESI(+)-MS spectrum for βCD:PNT (1:1), in which the ion of *m*/*z* 341 was ascribed to the protonated form of PNT, *i.e.* $[PNT+H]^+$, whereas *m*/*z* 171 was attributed to the doubly-charged species $[PNT+2H]^{2+}$. Moreover, the ions of *m*/*z* 467 and 1059 were attributed as the protonated ions formed between PNT and isethionate (ISO), *i.e.* $[PNT+ISO+H]^+$ and $[2PNT+3ISO+H]^+$, respectively. These PNT ions were observed in the ESI-MS spectrum of PNT (Fig. S2), confirming that free PNT molecules are in equilibrium with its ICs in aqueous solution. Moreover, these results indicated that the free PNT molecule is able to self-assemble, which was also observed in the PNT dilution curve by ITC. In addition to the free PNT ions, ICs were also observed in the ESI-MS spectrum of the βCD:PNT (1:1) system. Among these ions, there are observed those with *m*/*z* 1601, 738, and 1305. These ions were attributed as the protonated forms of the following ICs: $[\beta CD+PNT+ISO+H]^+$, $[\beta CD+PNT+2H]^{2+}$, and $[2\beta CD+PNT+2H]^{2+}$, respectively. At the

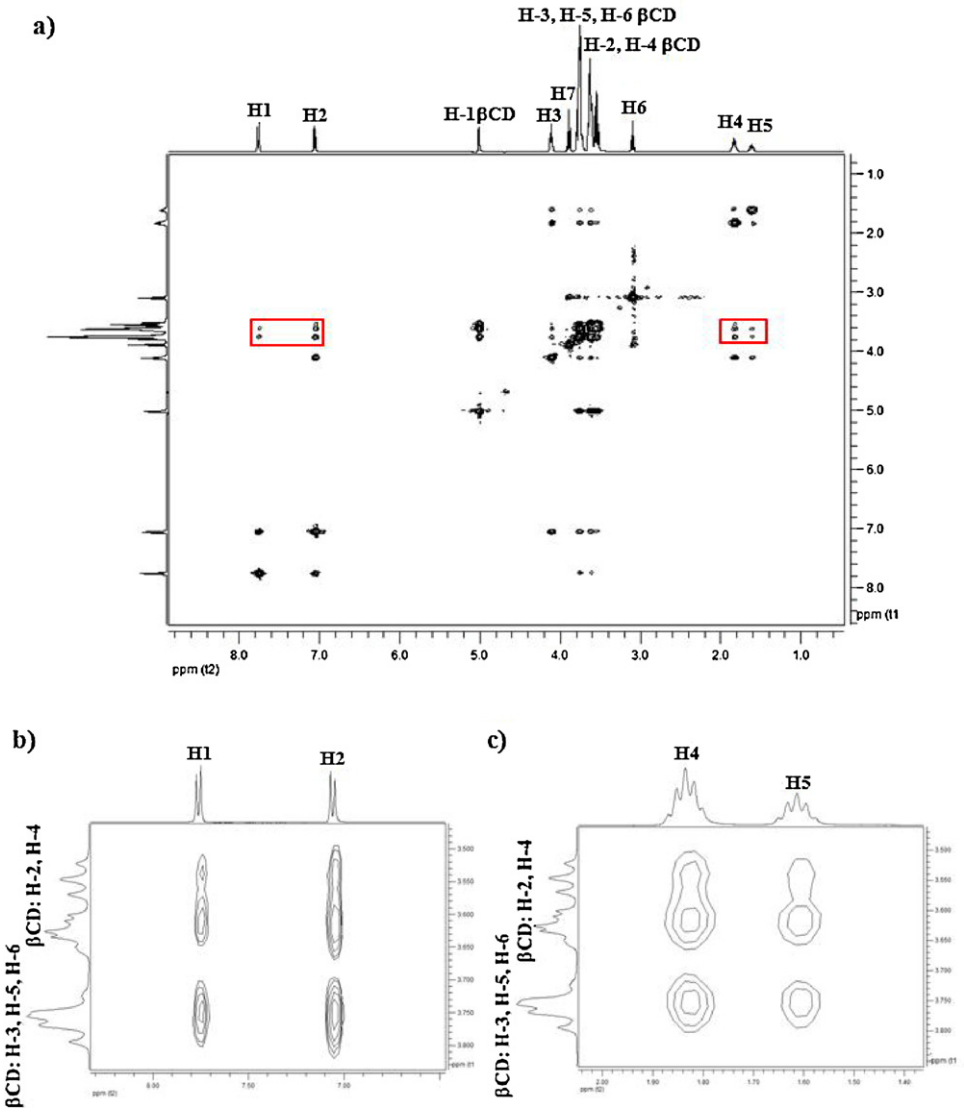

Fig. 3. (a) NMR 2D ROESY contour map (at 400 MHz) in D_2O of βCD:PNT (1:1) molar ratio and expansion of NMR 2D ROESY spectra of the βCD:PNT (1:1): (b) at δ 7.80–6.50 and (c) at δ 1.90–1.45.

molar ratio of (1:1), the PNT counter ion (ISO) was shifted from the molecule coordination sphere, when PNT interacted with the βCD, probably with its cavity forming ICs. This phenomenon is emphasized when the βCD:PNT (2:1) complex was formed in solution and ISO counter ion is not observed in the supramolecular structure, corroborating the NMR experiments. The 1:1 supramolecular complex detected in this experiment was $[\beta CD + PNT + ISO + H]^+$ and $[\beta CD + PNT + 2H]^{2+}$, in which the βCD also shifted the counter ion. The double charge molecular ions for βCD:PNT (1:1) system can be seen clearly in Fig. S3 of the Supplementary Material.

Fig. 4b displays the ESI-MS βCD:PNT at 2:1 molar ratio, in which the same ion peaks of Fig. 4a are presented. Moreover, the relative intensity of the *m*/*z* 1305 ion ($[2\beta CD + PNT + 2H]^{2+}$) is higher than that observed in Fig. 4a. This result indicates that the higher concentration of βCD induces the formation of greater amounts of this superstructure in solution. Additionally, the relative amount of $[\beta CD + PNT + ISO + H]^+$ is inferior to that observed in Fig. 4a. This trend is confirmed by the results from ESI-MS spectra at 3:1 and 4:1 βCD:PNT solutions, Fig. 4c and d respectively. Increasing the βCD concentration above 2:1 ratio, did

Table 1
^1H chemical shifts (at 400 MHz) of PNT protons of pure drug and in presence of βCD using D_2O and $\Delta\delta$ values.

Proton	δ PNT	$\delta_{\beta CD:PNT}$ (1:1)	$\Delta\delta$ 1:1/(βCD:PNT)	$\delta_{\beta CD:PNT}$ (2:1)	$\Delta\delta$ 2:1/(βCD:PNT)
H-1	7.60	7.77	−0.173	7.78	−0.180
H-2	6.98	7.07	−0.095	7.10	−0.125
H-3	4.01	4.11	−0.099	4.14	−0.126
H-4	1.73	1.84	−0.109	1.86	−0.128
H-5	1.49	1.63	−0.143	1.63	−0.139
H-6	3.01	3.10	−0.083	3.10	−0.082
H-7	3.81	3.89	−0.081	3.89	−0.080

$\Delta\delta = \delta_{PNT} - \delta_{\beta CD:PNT}$. Negative values indicate downfield shift.

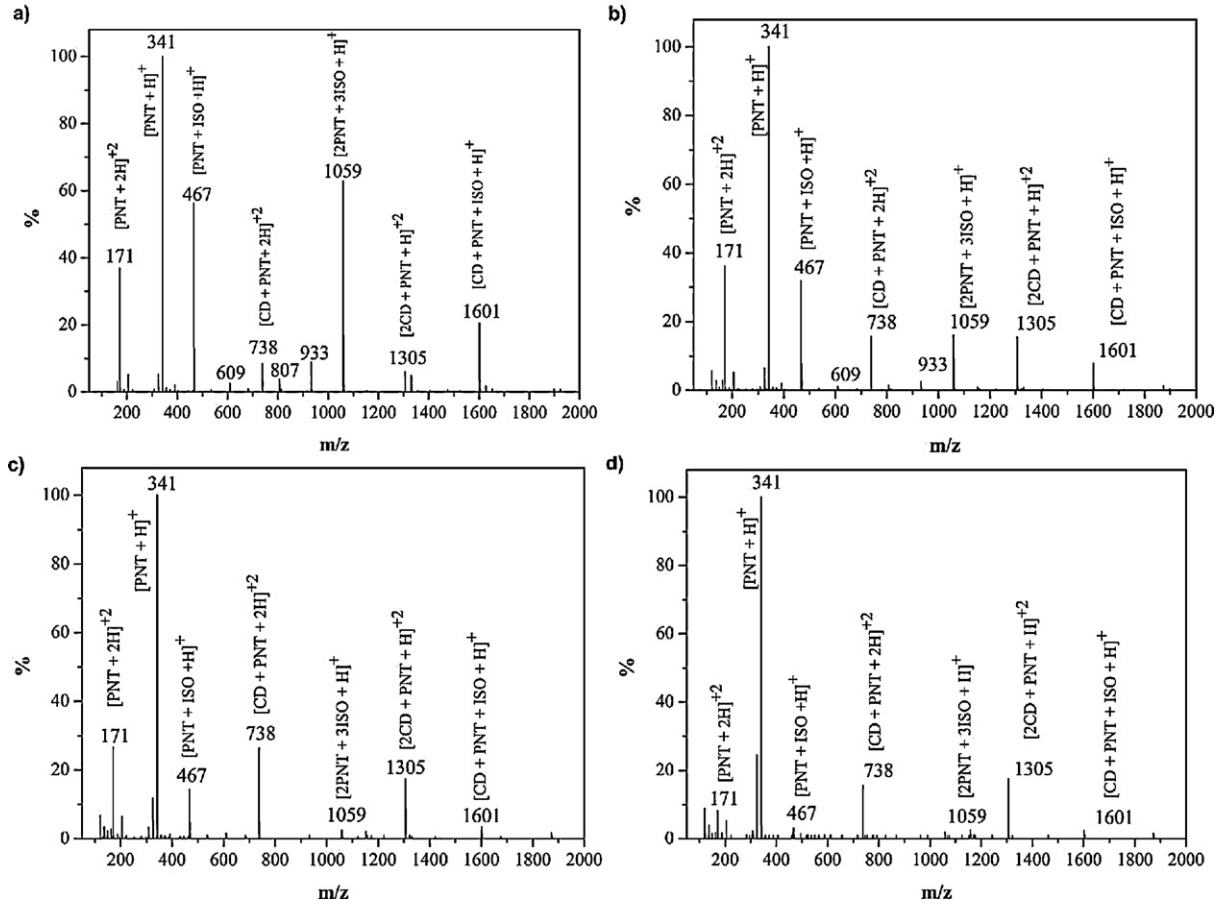

Fig. 4. ESI(+)-MS of an aqueous solution: (a) of β-cyclodextrin (βCD) and pentamidine isothionate (PNT ISO) in a molar proportion of 1:1, (b) βCD:PNT 2:1, (c) βCD:PNT 3:1 and (d) βCD:PNT 4:1.

not induced superstructures at 3:1, 4:1 or higher ratios of βCD :PNT. These results indicate that the most probable supramolecular species in equilibrium in aqueous solution are: free PNT molecule and its ICs at 1:1 and 2:1 molar ratio. This equilibrium is in accordance with those results obtained by ITC, in which a fractional (*N*) was observed. Moreover, when βCD concentration is increased from 1:1 molar ratio to 4:1, the relative amount of free PNT molecules such as $[PNT + ISO + H]^+$ and $[2PNT + 3ISO + H]^+$ are reduced in solution, suggesting that more supramolecular complexes (βCD:PNT at 1:1 and 2:1) are formed under the experimental conditions.

3.4. Fourier transform infrared spectroscopy (FTIR)

Infrared spectroscopy (FTIR) was used in order to characterize the ICs and associated with other techniques to suggest the inclusion process in the solid state. The vibrational spectra in the infrared region for the βCD, PNT, βCD:PNT (1:1) and PM-βCD:PNT (1:1) are shown in Fig. S4 in the Supplementary Material. Analyzing the βCD FTIR spectrum, its characteristics bands can be observed in accordance with the literature (Egyed, 1990; Teixeira et al., 2006; Rezende et al., 2009). The absorption spectrum in the infrared region for PNT exhibits well-defined bands and some vibrational modes can be highlighted, including the band observed at 3396 cm^{-1} which is attributed to the ν(OH) of the hydroxyl group of the isethionate counter ion and the bands observed at 3133 and 2952 cm^{-1}, respectively attributed to stretching of amidine (N—H) and aliphatic (C—H) groups. The bands observed at 1680 and 1488 cm^{-1} are respectively assigned to ν(CO) and ν(CC/CN), as described in the literature (Schmitz and Hubner, 1995).

Comparative analysis of the βCD:PNT (1:1) compound absorption spectrum (FTIR) with its precursors βCD and PNT demonstrated that PNT bands changed after interaction with the βCD, reducing the number of vibrational modes of free PNT indicating the lower mobility of PNT upon inclusion. In contrast, no change or reduction in the host and guest bands were observed in the PM-βCD:PNT (1:1) spectrum, indicating that PNT is not interacting with βCD in solid state for this system.

3.5. Thermal analysis (TG and DTA)

TG and DTA curves for the βCD:PNT (1:1), PM-βCD:PNT (1:1), βCD and PNT, are shown respectively in Figs. S5 and S6 in the Supplementary Material. The thermal profile of the βCD is in accordance with the literature (Yilmaz et al., 1995). Thermal analysis of the drug PNT can be seen in Fig. S5 (a) and shows a significant loss of mass in the range of 300–335 °C, attributed to its thermodegradation. It is observed in the DTA curve of the drug PNT, five endothermic events, including a peak at 192 °C corresponding to its melting point.

Thermogravimetric analysis for the βCD:PNT (1:1) indicated its higher thermal stability compared to the precursor and PM-βCD:PNT (1:1). In the TG curve of compound βCD:PNT (1:1) a weight loss of 7% is observed and was attributed to the loss of water molecules. The compound is stable up to 230 °C, where a decomposition stage begins and continues up to 246 °C with a mass loss

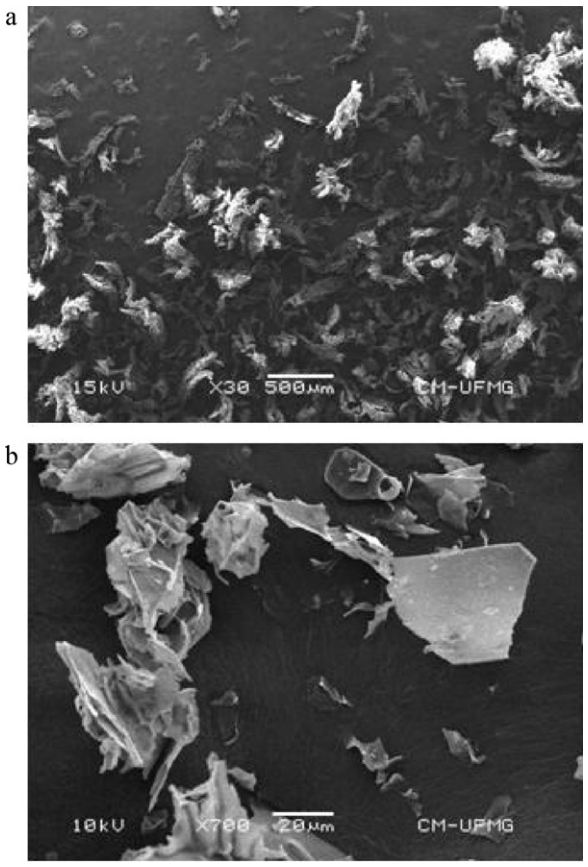

Fig. 5. SEM micrographs of (a) PNT at 30× and (b) βCD:PNT (1:1) at 700×.

of about 28%, which is related to the start of βCD thermodecomposition. Then, there is a third weight loss of 20% relative to the beginning of PNT thermodecomposition and at 340 °C there is 42% of residue. In the DTA curves, it is observed that the physical mixture thermal behavior is the sum of the thermal behaviors of free precursors βCD and PNT, unlike the inclusion complex βCD:PNT (1:1). The DTA curve of the compound βCD:PNT (1:1) does not show the endothermic peak of PNT fusion at 192 °C, unlike the physical mixture DTA curve in which endothermic events at 96, 192, 243 and 340 °C are observed. Moreover, the presence of only two events in the βCD:PNT (1:1) DTA curve, indicates a stronger interaction between the macromolecules βCD and drug and suggests the existence of a complex between βCD and PNT, indicating the existence of the inclusion compound βCD:PNT (1:1) in the solid state.

In addition, the thermal behavior of the βCD:PNT (2:1), βCD:PNT (3:1) and βCD:PNT (4:1) supramolecular systems did not differ from those observed at 1:1 molar ratio, indicating that the βCD concentration was not able to modify the PNT thermal stability.

3.6. Scanning electron microscopy (SEM)

Fig. 5 shows SEM images obtained for the free drug and the IC at βCD:PNT 1:1 molar ratio. Morphological analysis of the PNT indicates an amorphous profile and SEM images for the system βCD:PNT (1:1), Fig. 5b, exhibits a lamellar aspect and suggests that the IC is homogeneous in solid state. These lamellar forms are due to the sample freezing stage in liquid nitrogen, which anterior to the freeze drying process and the continuous drying process under vacuum.

Based on the results obtained in aqueous solution and in the solid state, PNT inclusion into the βCD cavity can be confirmed thus, *in vivo* experiments can be designed and PNT activity compared in the presence or absence of the host molecule administrated orally.

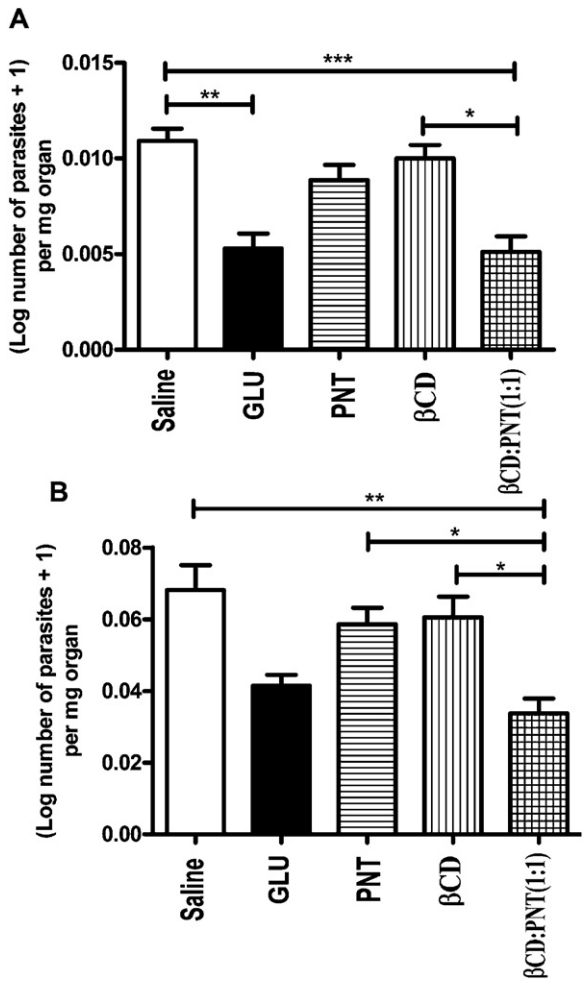

Fig. 6. Parasite burden in the liver (A) and spleen (B) of BALB/c mice infected with *L.* (*L.*) *infantum chagasi*. βCD:PNT (1:1) dose 145 mg/kg (contains 50 mg/kg of PNT and 95 mg/kg/day of βCD); free PNT dose 50 mg/kg, free CD dose 95 mg/kg/day; saline (negative control); GLU, commercial antimonial drug Glucantime® given intraperitoneally at 80 mg Sb/kg/day (positive control). Parasite burden was determined by limiting dilution assay. Data are shown as means ± SE ($n = 7–10$). The asterisks indicates that differences are statistically significant ($^{*}p < 0.05$, $^{**}p < 0.001$, $^{***}p < 0.0001$) according to Kruskal–Wallis test followed by Bonferroni post-test.

3.7. In vivo experiments

The results of *in vivo* experiments are shown in Fig. 6. Briefly, BALB/c mice were infected with *L. infantum chagasi* after treatment with βCD:PNT (1:1), free PNT, saline and both control experiments by oral route. From the analysis results, it was observed that both in liver and spleen showed no difference between the treated group with PNT at a dose of 50 mg/kg compared to the control group treated with saline solution, as expected since the said drug does not comprise an orally. However, as can be seen from the data, βCD:PNT (1:1) promoted a significant reduction of the parasite load in both organs, when compared to those in the control group treated with saline. The efficacy of orally-active βCD:PNT (1:1) was similar to that of the first-line glucantime treatment given parenterally, being these results in contrast with those obtained with orally administered PNT which did not induce a significant reduction of the parasite burden. Furthermore, the βCD:PNT (1:1) inclusion complex promoted a significantly lower parasite load in the spleen when compared to free PNT. The IC showed greater reduction of parasitemia in the liver in relation to the spleen.

The results, when considered in context, indicate enhanced oral activity of the βCD:PNT (1:1) when compared to free PNT in the murine model of visceral leishmaniasis and showed that the

encapsulation process of PNT with βCD alter the absorption characteristics of such drug, which makes this method a alternative promising for the treatment of leishmaniasis.

4. Conclusions

This work was carried out to gain a more complete comprehension concerning the non covalent interactions between PNT and βCD in aqueous solutions and the supramolecular structure of these ICs. Based on the results obtained from ITC, ESI-MS and NMR, sophisticated techniques to investigate the interactions in host–guest systems using CDs in aqueous solutions, we have demonstrated the PNT inclusion into the host cavity. ITC experiments allowed us to identify the thermodynamic parameters of the inclusion process and the stoichiometric coefficient indicated the equilibrium of more than one supramolecular system in aqueous solution. This observation was also verified through ESI-MS spectra of the ICs at 1:1, 2:1, 3:1 and 4:1 molar ratios. An interesting fact is that the IC at βCD:PNT (2:1) ratio showed a higher relative abundance compared to βCD:PNT (1:1). Additionally, molecular ions referring to the complex in the proportions 3:1 and 4:1 were not observed in the spectra.

Changes in chemical shift between free PNT and ICs hydrogen atoms, showed that increasing the βCD ratio in βCD:PNT (2:1) in the inclusion complex, does not alter the structure of the supramolecular system. 2D ROESY spectra allowed us to infer the depth inclusion of PNT in βCD cavity, since correlations were observed between both aromatic and aliphatic PNT hydrogen with βCD internal hydrogens. In this manner, all results suggest the formation of a βCD:PNT (1:1) supramolecular complex in equilibrium with a βCD:PNT (2:1) system, which suggests the formation of superstructures in solution. Moreover, the inclusion process was confirmed in the solid state using FTIR, TG/DTA and SEM.

Additionally, the biological assays showed a significant change in the characteristics of PNT in the presence of βCD, since the formulation administered *in vivo* in mice by gavage presented better oral activity, in contrast to free drug.

Acknowledgements

The authors would like to acknowledge the Brazilian agencies CNPq, CAPES, FAPEMIG (PRONEX 526/07) and Rede Mineira de Química (RQ-MG) for financial support and also INCT-Nanobiofar. ITC facility was supported by LNLS – Brazilian Synchrotron Light Laboratory/MCT.

Appendix A. Supplementary data

Supplementary data associated with this article can be found, in the online version, at http://dx.doi.org/10.1016/j.ijpharm.2012.09.039.

References

Akopyants, N.S., Kimblin, N., Secundino, N., Patrick, R., Peters, N., Lawyer, P., Dobson, D.E., Beverley, S.M., Sacks, D.L., 2009. Demonstration of genetic exchange during cyclical development of leishmania in the sand Fly vector. Science 324, 265–268.

Ashley, J.N., Barber, H.J., Ewins, A.J., Newbery, G., Self, A.D.H., 1942. Chemotherapeutic comparison of the trypanocidal action of some aromatic diamidines. J. Chem. Soc. 103–116.

Banerjee, G., Nandi, G., Mahato, S.B., Pakrashi, A., Basu, M.K., 1996. Drug delivery system: targeting of pentamidines to specific sites using sugar grafted liposomes. J. Antimicrob. Chemother. 38, 145–150.

Brewster, M.E., Loftsson, T., 2007. Cyclodextrins as pharmaceutical solubilizers. Adv. Drug Deliv. Rev. 59, 645–666.

Carrier, R.L., Miller, L.A., Ahmed, M., 2007. The utility of cyclodextrins for enhancing oral bioavailability. J. Control. Release 123, 78–99.

Charpentier, T.H., Wilder, P.T., Liriano, M.A., Varney, K.M., Pozharski, E., MacKerell, A.D., Coop, A., Toth, E.A., Weber, D.J., 2008. Divalent metal ion complexes of S100B in the absence and presence of pentamidine. J. Mol. Biol. 382, 56–73.

Chen, Y., Liu, Y., 2010. Cyclodextrin-based bioactive supramolecular assemblies. Chem. Soc. Rev. 39, 495–505.

Croft, S.L., Yardley, V., 2002. Chemotherapy of leishmaniasis. Curr. Pharm. Des. 8, 319–342.

Croft, S.L., Barrett, M.P., Urbina, J.A., 2005. Chemotherapy of trypanosomiases and leishmaniasis. Trends Parasitol. 21, 508–512.

De Sousa, F.B., Denadai, Â.M.L., Lula, I.S., Lopes, J.F., Dos Santos, H.F., De Almeida, W.B., Sinisterra, R.D., 2008a. Supramolecular complex of fluoxetine with beta-cyclodextrin: an experimental and theoretical study. Int. J. Pharm. 353, 160–169.

De Sousa, F.B., Denadai, Â.M.L., Lula, I.S., Nascimento, C.S., Fernandes, N.S.G., Lima, A.C., De Almeida, W.B., Sinisterra, R.D., 2008b. Supramolecular self-assembly of cyclodextrin and higher water soluble guest: thermodynamics and topological studies. J. Am. Chem. Soc. 130, 8426–8436.

De Sousa, F.B., Oliveira, M.F., Lula, I.S., Sansiviero, M.T.C., Cortes, M.E., Sinisterra, R.D., 2008c. Study of inclusion compound in solution involving tetracycline and beta-cyclodextrin by FTIR-ATR. Vib. Spectrosc. 46, 57–62.

De Sousa, F.B., Denadai, Â.M.L., Lula, I.S., Ianzer, D., Malaspina, E.R., de Camargo, A.C.M., dos Santos, R.A.S., Sinisterra, R.D., 2010. Structural and physical-chemical evaluation of Bradykinin potentiating peptide and its high soluble supramolecular complex. J. Inclusion Phenom. Macrocyclic Chem. 67, 407–422.

De Sousa, F.B., Lima, A.C., Denadai, Â.M.L., Anconi, C.P.A., De Almeida, W.B., Novato, W.T.G., Dos Santos, H.F., Drum, C.L., Langer, R., Sinisterra, R.D., 2012. Superstructure based on beta-CD self-assembly induced by a small guest molecule. Phys. Chem. Chem. Phys. 14, 1934–1944.

Denadai, Â.M.L., Teixeira, K.I., Santoro, M.M., Pimenta, A.M.C., Cortes, M.E., Sinisterra, R.D., 2007. Supramolecular self-assembly of beta-cyclodextrin: an effective carrier of the antimicrobial agent chlorhexidine. Carbohydr. Res. 342, 2286–2296.

Docampo, R., Moreno, S.N.J., 2003. Current chemotherapy of human African trypanosomiasis. Parasitol. Res. 90, S10–S13.

Duan, M.S., Zhao, N., Ossurardottir, I.B., Thorsteinsson, T., Loftsson, T., 2005. Cyclodextrin solubilization of the antibacterial agents triclosan and triclocarban: formation of aggregates and higher-order complexes. Int. J. Pharm. 297, 213–222.

Egyed, O., 1990. Spectroscopic studies on beta-cyclodextrin. Vib. Spectrosc. 1, 225–227.

Gibaud, S., Ben Zirar, S., Mutzenhardt, P., Fries, I., Astier, A., 2005. Melarsoprol-cyclodextrins inclusion complexes. Int. J. Pharm. 306, 107–121.

He, Y.F., Fu, P., Shen, X.H., Gao, H.C., 2008. Cyclodextrin-based aggregates and characterization by microscopy. Micron 39, 495–516.

Ivana Lula, F.B.d.S., Denadai, Â.M.L., Ianzer, D., de Camargo, A.C.M., Santos, R.A.S., Sinisterra, R.D., 2011. Study of the BPP7a peptide and its β-cyclodextrin complex: physicochemical characterization and complete sequence specific NMR assignments. J. Braz. Chem. Soc. 22, 1765–1773.

Lehn, J.M., 2002. Toward self-organization and complex matter. Science 295, 2400–2403.

Loftsson, T., Hreinsdottir, D., Masson, M., 2005. Evaluation of cyclodextrin solubilization of drugs. Int. J. Pharm. 302, 18–28.

Manfredi, R., Marinacci, G., Calza, L., Passarini, B., 2008. Diffuse cutaneous dissemination of visceral leishmaniasis during human immunodeficiency virus (HIV) infection, despite negligible immunodeficiency: repeated failure of liposomal amphotericin B administration, followed by successful long-term pentamidine and paromomycin administration. Int. J. Antimicrob. Agents 31, 590–592.

Marques, F.D., Ferreira, A.J., Sinisterra, R.D.M., Jacoby, B.A., De Sousa, F.B., Caliari, M.V., Silva, G.A.B., Melo, M.B., Nadu, A.P., Souza, L.E., Irigoyen, M.C.C., Almeida, A.P., Santos, R.A.S., 2011. An oral formulation of angiotensin-(1-7) produces cardioprotective effects in infarcted and isoproterenol-treated rats. Hypertension 57, 477–483.

Marques-da-Silva, E.A., Coelho, E.A.F., Gomes, D.C.O., Vilela, M.C., Masioli, C.Z., Tavares, C.A.P., Fernandes, A.P., Afonso, L.C.C., Rezende, S.A., 2005. Intramuscular immunization with p36(LACK) DNA vaccine induces IFN-gamma production but does not protect BALB/c mice against *Leishmania chagasi* intravenous challenge. Parasitol. Res. 98, 67–74.

Martins, P.S., Ochoa, R., Pimenta, A.M.C., Ferreira, L.A.M., Melo, A.L., da Silva, J.B.B., Sinisterra, R.D., Demicheli, C., Frezard, F., 2006. Mode of action of beta-cyclodextrin as an absorption enhancer of the water-soluble drug meglumine antimoniate. Int. J. Pharm. 325, 39–47.

Messner, M., Kurkov, S.V., Jansook, P., Loftsson, T., 2010. Self-assembled cyclodextrin aggregates and nanoparticles. Int. J. Pharm. 387, 199–208.

Murray, H.W., Berman, J.D., Davies, C.R., Saravia, N.G., 2005. Advances in leishmaniasis. Lancet 366, 1561–1577.

Nacher, M., Carme, B., Marie, D.S., Couppie, P., Clyti, E., Guibert, P., Pradinaud, R., 2001. Influence of clinical presentation on the efficacy of a short course of pentamidine in the treatment of cutaneous leishmaniasis in French Guiana. Ann. Trop. Med. Parasitol. 95, 331–336.

Nakayama, H., Loiseau, P.M., Bories, C., de Ortiz, S.T., Schinini, A., Serna, E., de Arias, A.R., Fakhfakh, M.A., Franck, X., Figadere, B., Hoequemiller, R., Fournet, A., 2005. Efficacy of orally administered 2-substituted quinolines in experimental murine cutaneous and visceral leishmaniases. Antimicrob. Agents Chemother. 49, 4950–4956.

Passos, J.J., De Sousa, F.B., Lula, I.S., Barreto, E.A., Lopes, J.F., De Almeida, W.B., Sinisterra, R.D., 2011. Multi-equilibrium system based on sertraline and β-cyclodextrin supramolecular complex in aqueous solution. Int. J. Pharm. 421, 24–33.

Paul, M., Fessi, H., Laatiris, A., Boulard, Y., Durand, R., Deniau, M., Astier, A., 1997. Pentamidine-loaded poly(D,L-lactide) nanoparticles: physicochemical properties and stability work. Int. J. Pharm. 159, 223–232.

Paul, M., Durand, R., Boulard, Y., Fusai, T., Fernandez, C., Rivollet, D., Deniau, M., Astier, A., 1998. Physicochemical characteristics of pentamidine-loaded polymethacrylate nanoparticles: implication in the intracellular drug release in Leishmania major infected mice. J. Drug Target. 5, 481–490.

Piotto, M., Saudek, V., Sklenar, V., 1992. Gradient-tailored excitation for single-quantum Nmr-spectroscopy of aqueous-solutions. J. Biomol. NMR 2, 661–665.

Puckowska, A., Bielawski, K., Bielawski, A., Midura-Nowaczek, K., 2004. Aromatic analogues of DNA minor groove binders – synthesis and biological evaluation. Eur. J. Med. Chem. 39, 99–105.

Rezende, B.A., Cortes, S.F., De Sousa, F.B., Lula, I.S., Schmitt, M., Sinisterra, R.D., Lemos, V.S., 2009. Complexation with beta-cyclodextrin confers oral activity on the flavonoid dioclein. Int. J. Pharm. 367, 133–139.

Schmitz, H.U., Hubner, W., 1995. Comparative-study of berenil-poly-nucleotide and pentamidine-poly-nucleotide complexes using UV/vis and FTIR spectroscopy. Biospectroscopy 1, 275–289.

Schneider, H.J., Hacket, F., Rudiger, V., Ikeda, H., 1998. NMR studies of cyclodextrins and cyclodextrin complexes. Chem. Rev. 98, 1755–1785.

Siddiqui, R., Syed, A., Tomas, S., Prieto-Garcia, J., Khan, N.A., 2009. Effect of free versus liposomal-complexed pentamidine isethionate on biological characteristics of *Acanthamoeba castellanii* in vitro. J. Med. Microbiol. 58, 327–330.

Sklenar, V., Piotto, M., Leppik, R., Saudek, V., 1993. Gradient-tailored water suppression for H-1-N-15 Hsqc experiments optimized to retain full sensitivity. J. Magn. Reson. Ser. A 102, 241–245.

Szejtli, J., 1998. Introduction and general overview of cyclodextrin chemistry. Chem. Rev. 98, 1743–1753.

Teixeira, L.R., Sinisterra, R.D., Vieira, R.P., Scarlatelli-Lima, A., Moraes, M.F.D., Doretto, M.C., Denadai, A.M., Beraldo, H., 2006. An inclusion compound of the anticonvulsant sodium valproate into alpha-cyclodextrin: physico-chemical characterization. J. Inclusion Phenom. Macrocyclic Chem. 54, 133–138.

Turnbull, W.B., Daranas, A.H., 2003. On the value of c: can low affinity systems be studied by isothermal titration calorimetry? J. Am. Chem. Soc. 125, 14859–14866.

Wenz, G., Han, B.H., Muller, A., 2006. Cyclodextrin rotaxanes and polyrotaxanes. Chem. Rev. 106, 782–817.

Yilmaz, V.T., Karadag, A., Icbudak, H., 1995. Thermal-decomposition of beta-cyclodextrin inclusion complexes of ferrocene and their derivatives. Thermochim. Acta 261, 107–118.

Zolek, T., Maciejewska, D., 2010. Theoretical models of pentamidine analogs activity based on their DNA minor groove complexes. Eur. J. Med. Chem. 45, 1991–1999.